ARTICLE
Journal of Cellular Biochemistry 113:465–472 (2012)

Journal of Cellular Biochemistry

In Vivo Imaging of Nuclear-Cytoplasmic Deformation and Partition During Cancer Cell Death Due to Immune Rejection

Yasuyuki Amoh,[1,2,3] Yuko Hamada,[3] Kensei Katsuoka,[3] and Robert M. Hoffman[1,2*]

[1] *AntiCancer, Inc., 7917 Ostrow Street, San Diego, California 92111*

[2] *Department of Surgery, University of California San Diego, California 92103*

[3] *Department of Dermatology, Kitasato University School of Medicine, Minami Ward, Sagamihara 252-0373, Japan*

ABSTRACT

In this report, we investigated the in vivo cell biology of cancer cells during immune rejection. The use of nestin-driven green fluorescent protein (ND-GFP) transgenic mice as hosts, in which nascent blood vessels express GFP, and implanted dual-color mouse mammary tumor 060562 (MMT) cells, in which the cytoplasm expresses red fluorescent protein (RFP) and the nuclei express GFP, allowed very important novel observations of angiogenesis and subcellular death pathways during immune rejection of a tumor. Nascent blood vessels did not form in the initially-growing mouse mammary tumor in ND-GFP immunocompetent mice. In contrast, in ND-GFP immunodeficient nude mice, numerous GFP-expressing nascent blood vessels grew into the tumor. The results suggest that insufficient nascent tumor angiogenesis was important in tumor rejection. During immune rejection, the cancer cells deformed their cytoplasm and nuclei, which were readily imaged by RFP and GFP, respectively. The nuclear membrane of the cancer cells ruptured, and chromatin extruded during partition of cytoplasm and nuclei. T lymphocytes infiltrated into the initially-growing tumor in the nestin-GFP transgenic immunocompetent mice. The cytotoxic role of the sensitized T lymphocytes was confirmed in vitro when they were co-cultured with MMT cells. The CD8a-positive lymphocytes attached to the cancer cells and caused nuclear condensation, deformation, and partition from their cytoplasm, similar to what occurred in vivo. The color-coded subcellular fluorescence-imaging model of immune rejection of cancer cells can provide a comprehensive system for further testing of immune-based treatment for cancer. J. Cell. Biochem. 113: 465–472, 2012.

KEY WORDS: GFP; RFP; NUCLEUS; CYTOPLASM; NESTIN; TRANSGENIC MICE; IMMUNOCOMPETENT MICE; NUDE MICE; IMMUNE REJECTION; SUBCELLULAR IN VIVO IMAGING; NUCLEAR-CYTOPLASMIC DYNAMICS; CELL DEATH; APOPTOSIS

The use of fluorescent proteins to differentially label cancer calls in the nucleus and cytoplasm and high-powered imaging technology has now enabled visualization of the nuclear-cytoplasmic dynamics of cancer cells in vivo as well as in vitro [Yamamoto et al., 2004; Jiang et al., 2006; Hoffman, 2005].

ORIGINS OF SUBCELLULAR IMAGING IN VIVO

Subcellular imaging in vivo became feasible when our laboratory engineered dual-color fluorescent cells with GFP in the nucleus and red fluorescent protein (RFP) in the cytoplasm. To obtain the dual-color cells, RFP was expressed in the cytoplasm of cancer cells, and GFP, linked to histone H2B, was expressed in the nucleus. Nuclear GFP expression enabled visualization of nuclear dynamics, whereas simultaneous cytoplasmic RFP expression enabled visualization of nuclear-cytoplasmic ratios as well as cell and nuclear shape changes. The cell-cycle position of individual living cells was readily visualized by the nuclear-cytoplasmic ratio and nuclear morphology. Real-time induction of apoptosis was observed by nuclear size changes and progressive nuclear fragmentation [Yamamoto et al., 2004; Jiang et al., 2006].

SUBCELLULAR IMAGING OF CANCER CELL DEFORMATION IN CAPILLARIES

The dual-color cells, with GFP in the nucleus and RFP in the cytoplasm, were used to visualize the cytoplasmic and nuclear dynamics of cells migrating in capillaries. Highly-deformed cancer cells containing elongated nuclei in capillaries in a skin flap were imaged in living mice. The cells and nuclei in the capillaries elongated to fit the width of narrow capillaries [Yamauchi et al., 2005].

IMAGING CANCER CELL TRAFFICKING IN BLOOD VESSELS

The nuclear and cytoplasmic behavior of cancer cells was imaged in real time in larger blood vessels as they moved by various means or adhered to the vessel surface in an abdominal skin flap. During extravasation, real-time dual-color imaging showed that

*Correspondence to: Robert M. Hoffman, Ph.D., AntiCancer, Inc., 7917 Ostrow Street, San Diego, CA 92111.
E-mail: all@anticancer.com

Received 9 September 2011; Accepted 12 September 2011 • DOI 10.1002/jcb.23370 • © 2011 Wiley Periodicals, Inc.
Published online 21 September 2011 in Wiley Online Library (wileyonlinelibrary.com).

cytoplasmic processes of the cancer cells exited the vessels first, with nuclei following along the cytoplasmic projections. Both cytoplasm and nuclei underwent deformation during extravasation [Yamauchi et al., 2005].

IMAGING CANCER CELL TRAFFICKING IN LYMPHATIC VESSELS

Dual-color cancer cells were used to visualize real-time imaging of cancer-cell trafficking in lymphatic vessels. Dual-color cells were injected into the inguinal lymph node of nude mice. The labeled cancer cells trafficked through lymphatic vessels where they were imaged via a skin flap in real time at the cellular level until they entered the axillary lymph node [Hayashi et al., 2007].

NONINVASIVE IMAGING OF TUMOR–STROMA INTERACTION AT THE CELLULAR AND SUBCELLULAR LEVEL

To noninvasively image cancer-cell/stromal-cell interaction in the tumor microenvironment and drug response at the cellular level in live animals in real time, we developed a new imageable three-color animal model. The model consisted of nude mice, ubiquitously expressing GFP, transplanted with dual-color cancer cells labeled with GFP in the nucleus and RFP in the cytoplasm. The Olympus IV100 Laser Scanning Microscope, with ultra-narrow microscope objectives ("stick objectives"), was used for noninvasive three-color imaging of the two-color cancer cells interacting with the GFP-expressing stromal cells of the host mouse. In this model, drug response of both cancer and stromal cells in the intact live animal was also imaged in real time. Various in vivo phenomena of tumor–host interaction and cellular dynamics were noninvasively imaged, including mitotic and apoptotic tumor cells, stromal cells interacting with the tumor cells, tumor vasculature, and tumor blood flow [Yang et al., 2004, 2007].

STROMAL CELLS ARE NECESSARY FOR METASTASIS

The role of host cells in tumor progression and metastasis is critical. After splenic injection, in GFP mice, of dual-color human colon cancer cells, expressing GFP in the nucleus and RFP in the cytoplasm, splenocytes, expressing GFP, co-trafficked with the cancer cells to the liver and facilitated metastatic colony formation. When the dual-color cancer cells were injected into the portal vein, all the cancer cells died. In contrast, splenic injection of cells resulted in the aggressive formation of liver and distant metastasis. When GFP spleen cells and RFP cancer cells were co-injected in the PV, RFP liver metastasis resulted that contained GFP spleen cells. These results suggest a novel interaction whereby passenger stromal cells, in this case splenocytes, were necessary for formation of liver metastasis [Bouvet et al., 2006]. Our result, that stromal cells are necessary for metastasis, was recently confirmed using a lung cancer model [Duda et al., 2010].

PRE-TREATMENT OF MICE WITH CYCLOPHOSPHAMIDE INCREASES VIABILITY OF CANCER CELLS SUBSEQUENTLY INJECTED

Cancer cells, labeled in the nucleus with GFP and RFP in the cytoplasm, were injected via various routes in nude mice. Twenty-four hours before cancer cell injection, cyclophosphamide was given i.p. In cyclophosphamide pre-treated mice, proliferation and extravasation occurred along with extravascular colony formation. In the nonpretreated mice, most cancer cells remained quiescent in vessels without extravasation or died. Cyclophosphamide did not directly affect the cancer cells because cyclophosphamide was cleared by the time the cancer cells were injected. Thus, cyclophosphamide can sometimes enhance critical steps in malignancy rather than inhibit them [Tsuji et al., 2006].

In the present report, the use of nestin-driven green fluorescent protein (ND-GFP) transgenic mice as hosts, in which nascent blood vessels express GFP and dual-color mouse mammary tumor (MMT) cells, in which the cytoplasm expresses RFP and the nuclei express GFP, allowed very important novel angiogenesis and subcellular death pathway observations to be made during immune rejection of a tumor.

MATERIALS AND METHODS

ND-GFP TRANSGENIC IMMUNOCOMPETENT MICE AND ND-GFP TRANSGENIC NUDE MICE

Transgenic mice, carrying GFP under the control of the nestin promoter, were used [Li et al., 2003; Amoh et al., 2004, 2005]. The ND-GFP gene was crossed into nude mice on the C57BL/6 background to produce ND-GFP transgenic nude mice [Amoh et al., 2005].

PRODUCTION OF RFP AND HISTONE H2B-GFP RETROVIRUS

For RFP retrovirus production, The *Hin*d III/*Not* I fragment from pDsRed2 containing the full-length RFP cDNA, was inserted into the *Hin*d III/*Not* I site of pLNCX2 that has the neomycin resistance gene to establish the pLNCX2-DsRed2 plasmid. For vector production, PT67 packaging cells, at 70% confluence, were incubated with a precipitated mixture of LIPOFECTAMINE™ reagent and saturating amounts of pLNCX2-DsRed2 plasmid. The cells were examined by fluorescence microscopy 48 h post-transduction. For selection of a clone producing high amounts of a RFP retroviral vector (PT67-DsRed2), the cells were cultured in the presence of 200–1,000 μg/ml G418, increased in a stepwise manner.

For histone H2B-GFP, the histone H2B gene was ligated to the 5′ end of GFP gene. The histone H2B-GFP fusion gene was inserted at the *Hind* III/*Cal* I site of the pLHCX that has the hygromycin resistant gene to form the pLHCX histone H2B-GFP plasmid. To establish a clone producing high amounts of the histone H2B-GFP retroviral vector, the pLHCX histone H2B-GFP plasmid was transfected to PT67 packaging cells by the same method for PT67-DsRed2. The transfected cells were cultured in the presence of 200–400 μg/ml of hygromicyn increased stepwise [Hoffman and Yang, 2006].

RFP AND HISTONE H2B-GFP GENE TRANSDUCTION OF MOUSE MAMMARY TUMOR 060562 (MMT) CELLS

To establish dual-color cells, clones of MMT cells expressing RFP in the cytoplasm (MMT RFP), were initially established. Briefly, MMT cells were incubated with a 1:1 precipitated mixture of retroviral supernatants of PT67-RFP cells for 72 h. Fresh medium was replenished at this time. Cells were harvested with trypsin/EDTA 72 h post-transduction. The cells were subcultured at a ratio of 1:15 into selective medium, which contained 200 μg/ml of G418. The level of G418 was increased stepwise up to 800 μg/ml. MMT-RFP cells were isolated with cloning cylinders using trypsin/EDTA and

amplified by conventional culture methods. For establishing dual-color cells, MMT-RFP cells were incubated with a 1:1 precipitated mixture of retroviral supernatants of PT67-histone H2B-GFP cells and culture medium. To select the double transformants, cells were incubated with hygromycin 72 h after transfection and the level of hygromycin was increased stepwise up to 400 μg/ml. The cells were examined by fluorescence microscopy and bright MMT dual-color clones were isolated with cloning cylinders [Hoffman and Yang, 2006].

ORTHOTOPIC IMPLANTATION OF TUMOR CELLS

ND-GFP transgenic immunocompetent mice and ND-GFP transgenic nude mice (6–8 week-old females) were used. Twenty microliters, containing 5×10^5 RFP-expressing MMT or dual-colored MMT cells per mouse, were injected in the mammary fat pad with a 1 ml 27G1/2 latex-free syringe (Becton Dickinson). The mice were anesthetized with tribromoethanol (i.p. injection of 0.2 ml/10 g body weight using a 1.2% solution).

CANCER CELL–LYMPHOCYTE INTERACTION IN VITRO

ND-GFP transgenic female immunocompetent mice, 6–8 weeks, were used. Twenty microliters, containing 5×10^5 dual-colored MMT cells, were injected in the mammary fat pad two times, with a 1-week interval. The mice were anesthetized with tribromoethanol. The draining lymph node was excised, and the cells from the draining lymph node were removed 1 week after the last cancer-cell injection. Lymph nodes were similarly removed from non-tumor-bearing mice. Lymphocyte suspensions were prepared by gentle teasing of the lymph node. The cells were washed three times with PBS. Lymphocytes ($5 \times 10^5\ ml^{-1}$) were incubated with MMT cancer cells ($5 \times 10^4\ ml^{-1}$). The MMT cells and the immunized or nonimmunized lymphocytes were cultured in 24-well tissue culture

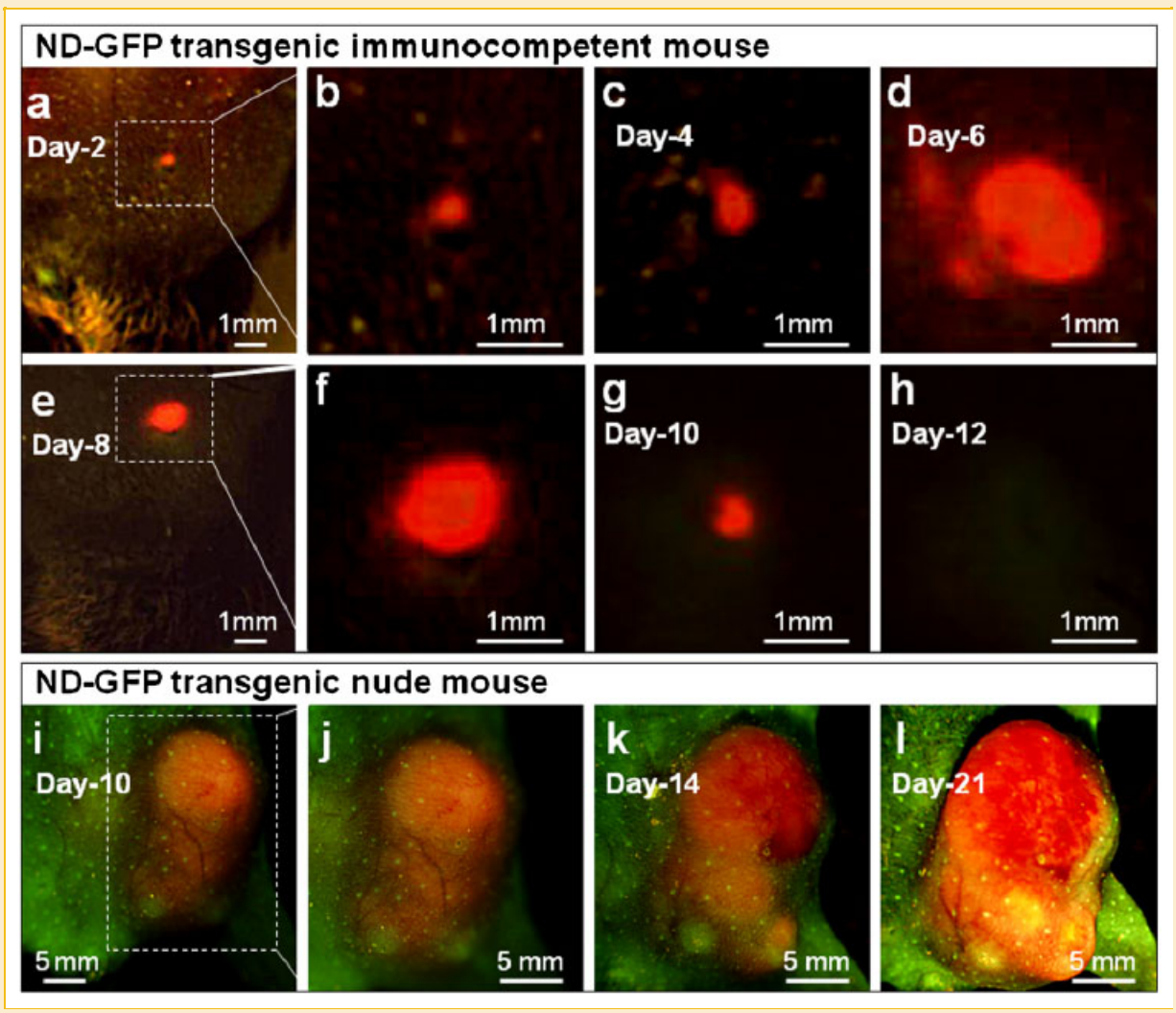

Fig. 1. a–h: RFP-expressing mouse mammary tumor 060562 (MMT) cells were injected orthotopically in nestin-driven (ND-GFP) transgenic immunocompetent mice. After day-8, the initially-growing RFP-expressing MMT tumor spontaneously regressed. After day-12, the tumor spontaneously eradicated. b,f: Higher magnifications of areas of (a,e) indicated by the white dashed boxes. i–l: RFP-expressing MMT cells were injected orthotopically in ND-GFP transgenic nude mice. In the ND-GFP transgenic nude mice, the RFP-expressing MMT tumor continued to grow. j: Higher magnification of area of (i) indicated by the white dashed box.

dishes (Corning, Aliso Viejo, CA) with RPMI 1640 medium (Cellgro, Herndon, VA) containing 10% fetal bovine serum (FBS) in a 37°C, 5% CO_2 tissue-culture incubator. After 24, 48, and 72 h, the MMT cell–lymphocyte interaction was directly observed by fluorescence microscopy.

IMMUNOHISTOCHEMICAL STAINING

Co-localization of ND-GFP fluorescence and CD31 (BD Pharmingen, San Diego, CA) in frozen skin sections of the ND-GFP transgenic nude mice was detected with the anti-rat immunoglobulin horseradish peroxidase detection kit (BD Pharmingen) was used following the manufacturer's instructions. For lymphocyte staining, the primary antibodies used were anti-CD3ε mAb (1:10; BD Pharmingen), anti-CD8a (Ly-2) mAb (1:10; BD Pharmingen), and anti-granzyme B mAb (1:100; Lab Vision, Fremont, CA). Substrate-chromogen 3,3′-diaminobenzidine staining was used for antigen staining.

FLUORESCENCE MICROSCOPY

Fluorescence microscopy was with an Olympus IMT-2 inverted microscope equipped with a mercury lamp power supply. The microscope had a GFP filter set (Chroma Technology, Brattleboro, VT).

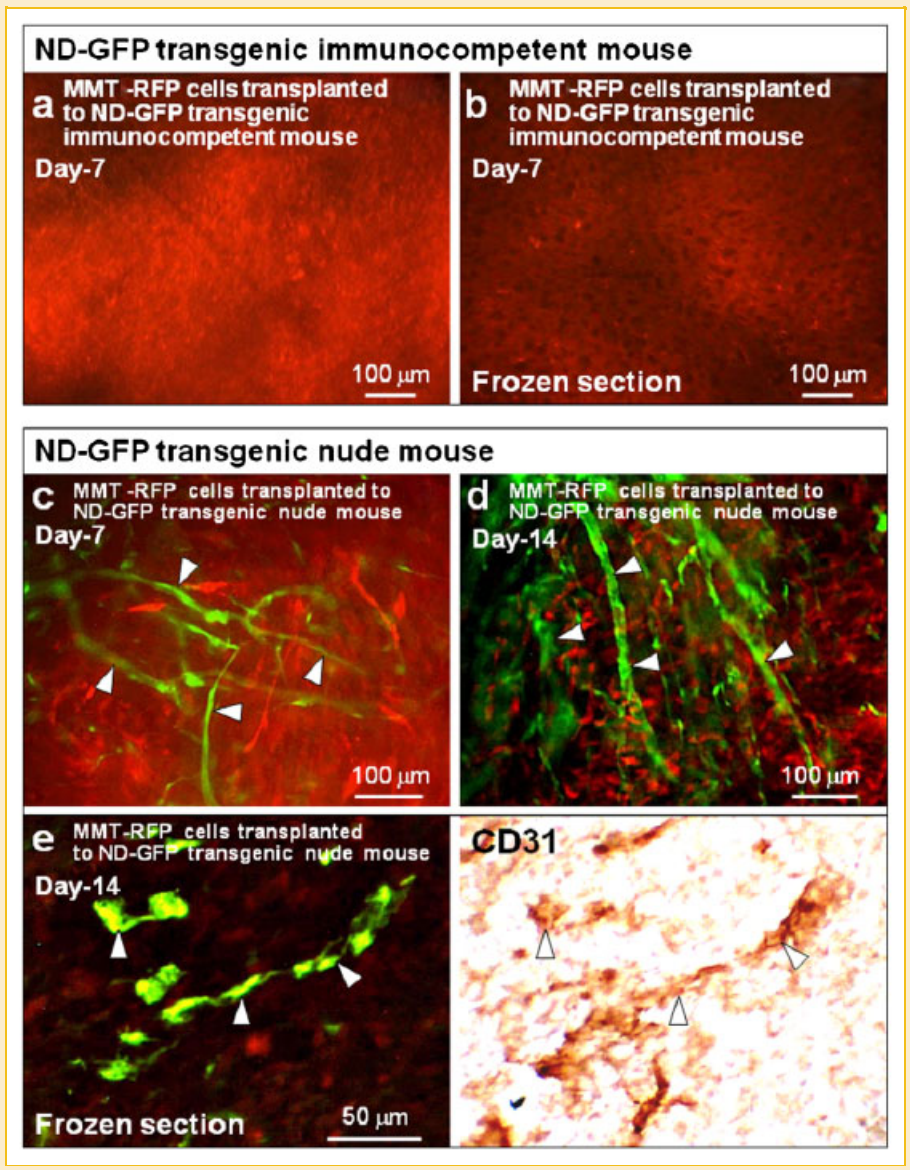

Fig. 2. a,b: Day-7 after orthotopic injection of RFP-expressing MMT cells in ND-GFP transgenic immunocompetent mice. Nascent GFP-expressing blood vessels were not observed. b: Frozen section. c,d: Day-7 (c) and -14 (d). After orthotopic injection of RFP-expressing MMT cells in ND-GFP transgenic immunodeficient nude mice, newly formed ND-GFP-expressing nascent blood vessels (white arrowheads) were imaged growing into the tumor. e: Immunohistochemical staining showed that CD31 and ND-GFP fluorescence were positive in the newly formed ND-GFP-expressing blood vessels (white arrowheads).

RESULTS AND DISCUSSION

REGRESSION OF MOUSE MAMMARY TUMOR 060562 (MMT) BREAST CANCER IN THE ND-GFP TRANSGENIC IMMUNOCOMPETENT MICE

RFP-expressing MMT cells were injected orthotopically in ND-GFP transgenic immunocompetent mice. After day-8, the RFP-expressing MMT tumor spontaneously regressed. By day-12, the tumor had been spontaneously eradicated (Fig. 1a–h). In contrast, when RFP-expressing MMT cells were injected orthotopically in the ND-GFP transgenic nude mice, the RFP-expressing MMT tumor grew continuously (Fig. 1i–l).

LACK OF TUMOR ANGIOGENESIS IN IMMUNOCOMPETENT HOSTS

At day-7 after orthotopic injection of RFP-expressing MMT cells in ND-GFP transgenic immunocompetent mice, nascent blood vessels were not observed in the initially-growing tumor (Fig. 2a,b). In contrast, at days 7 and 14 after orthotopic injection of RFP-expressing

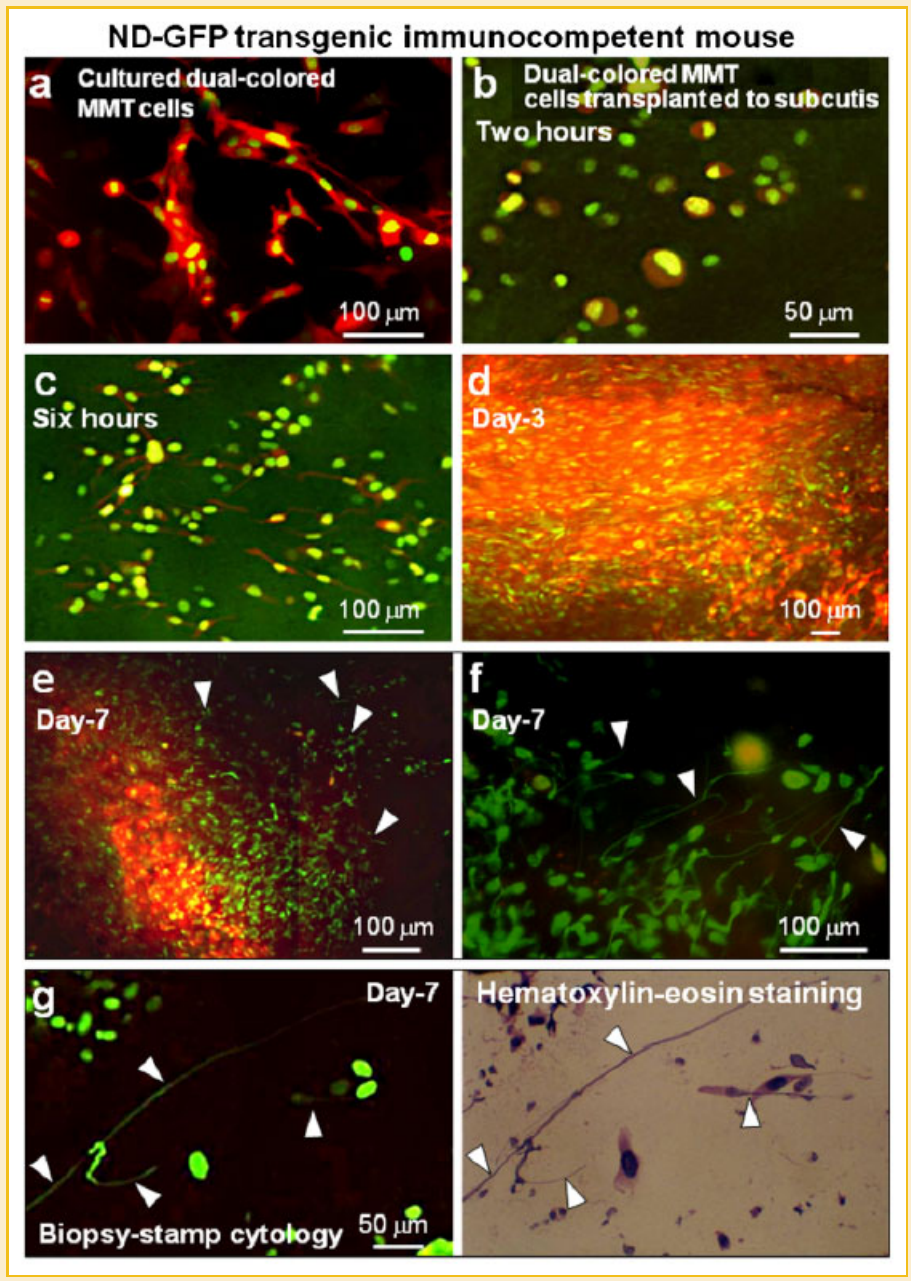

Fig. 3. a: Cultured dual-colored MMT cells with RFP expression in the cytoplasm, and GFP linked to histone H2B, expressed in the nuclei. b: Two hours after transplantation of the dual-colored MMT cells to ND-GFP transgenic immunocompetent mice. c: After 6 h, the dual-color MMT cells had elongated cytoplasms. d: At day-3, the dual-color MMT cells were observed growing in the central area of the tumor in ND-GFP transgenic immunocompetent mice. e,f: At day-7, the nuclei and cytoplasm of the dual-colored MMT cells partitioned. Extruded chromatin was spread thread-like (white arrowheads). g: The extruded thread-like nuclear material was hematoxylin-positive (white arrowheads).

MMT cells in ND-GFP transgenic nude mice, newly formed ND-GFP-expressing nascent blood vessels were growing into the tumor (Fig. 2c,d). IHC staining showed that CD31 and ND-GFP fluorescence were positive in the newly formed ND-GFP-expressing blood vessels (Fig. 2e).

IMAGING CANCER-CELL NUCLEAR-CYTOPLASMIC DYNAMICS DURING IMMUNE REGRESSION

Dual-colored MMT cells, with RFP expressed in the cytoplasm and GFP linked to histone H2B expressed in the nuclei, were transplanted in the mammary fatpad of ND-GFP transgenic immunocompetent

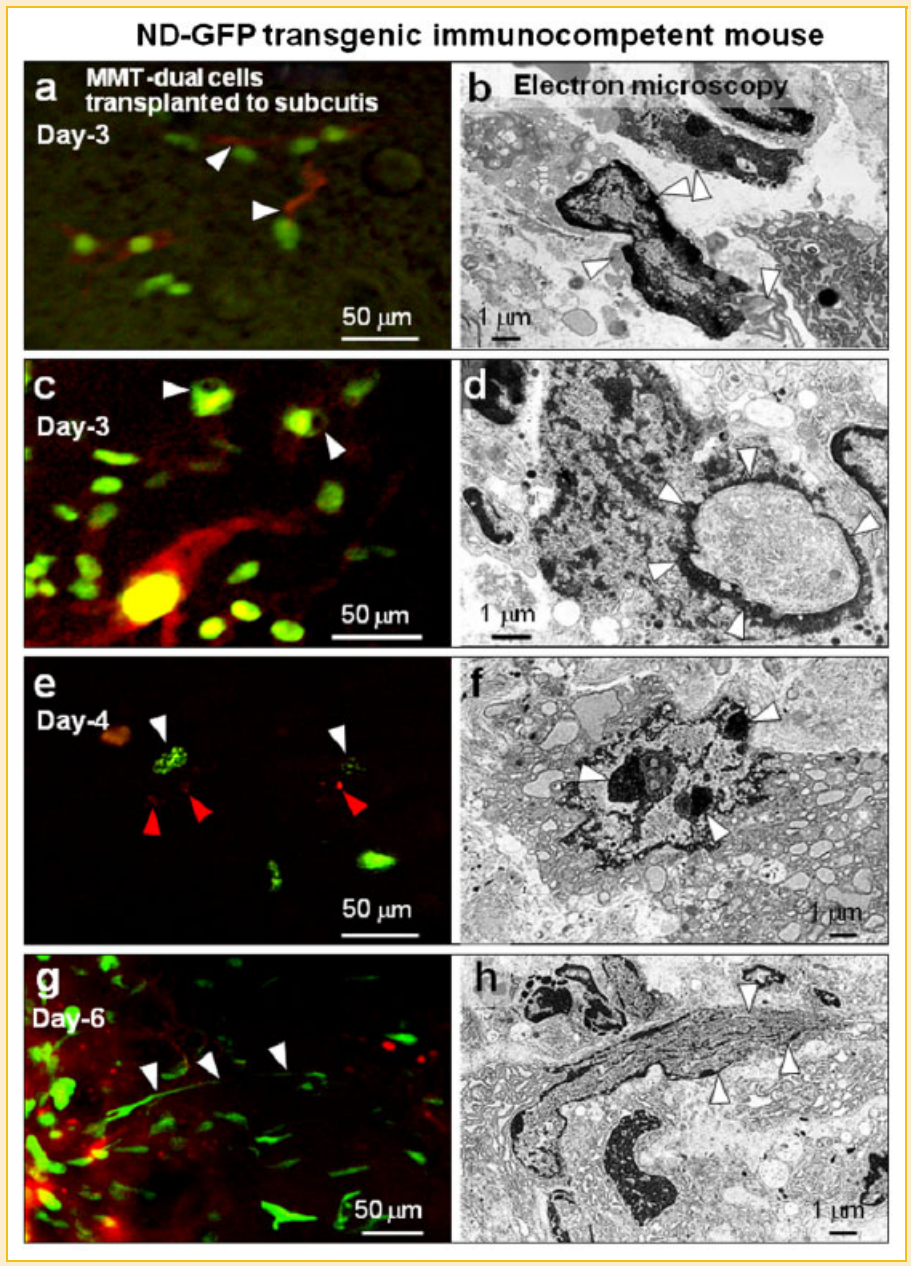

Fig. 4. a,b: At day-3, after transplantation of dual-color MMT cells, expressing RFP in the cytoplasm and GFP in the nuclei, to ND-GFP immunocompetent mice, the RFP-expressing cytoplasm partitioned from the GFP-expressing nuclei in the peripheral area of the tumor white arrowheads). b: Transmission electron microscopy showed partition of cancer cell cytoplasm and nuclei (white arrowheads). c,d: At day-3 after transplantation, ring-shaped GFP-expressing chromatin condensation was observed (white arrowheads). d: Transmission electron microscopy also showed ring-shaped chromatin condensation (white arrowheads). e,f: At day-4 after transplantation, apoptotic cells in the tumor were observed. GFP-expressing nuclei (white arrowheads) and RFP-expressing cytoplasm (red arrowheads) were imaged. f: Transmission electron microscopy demonstrated apoptotic characteristics of the cancer cells including chromatin condensation, nuclear fragmentation, and apoptotic body formation (white arrowheads). g,h: At day-6 after transplantation, GFP nuclei partitioned from the RFP-expressing cytoplasm. The extruded nuclei had thread-like structures of chromatin (white arrowheads). h: The cancer cells contained irregularly elongated nuclei. The nuclear membranes of the cancer cells ruptured, and nuclear material extruded (white arrowheads).

mice. After 6 h, the RFP-expressing cytoplasm of the cancer cells elongated. At day-3, dual-colored MMT cells were observed growing in the central area of the tumor. At day-7, partition of GFP nuclei and RFP cytoplasm of the MMT cells was observed. The partitioned nuclei generated long threads of chromatin. The thread-like nuclear material was hematoxylin-positive (Fig. 3). At day-3, the partition of RFP-expressing cytoplasm from the GFP-expressing nuclei of the dual-color MMT cells was also observed in the peripheral area of the tumor. Transmission electron microscopy also showed cancer cell cytoplasm partitioned from the nuclei (Fig. 4a,b). At day-3, ring-shaped chromatin condensation was observed by GFP fluorescence in the tumor. Transmission electron microscopy also showed cancer

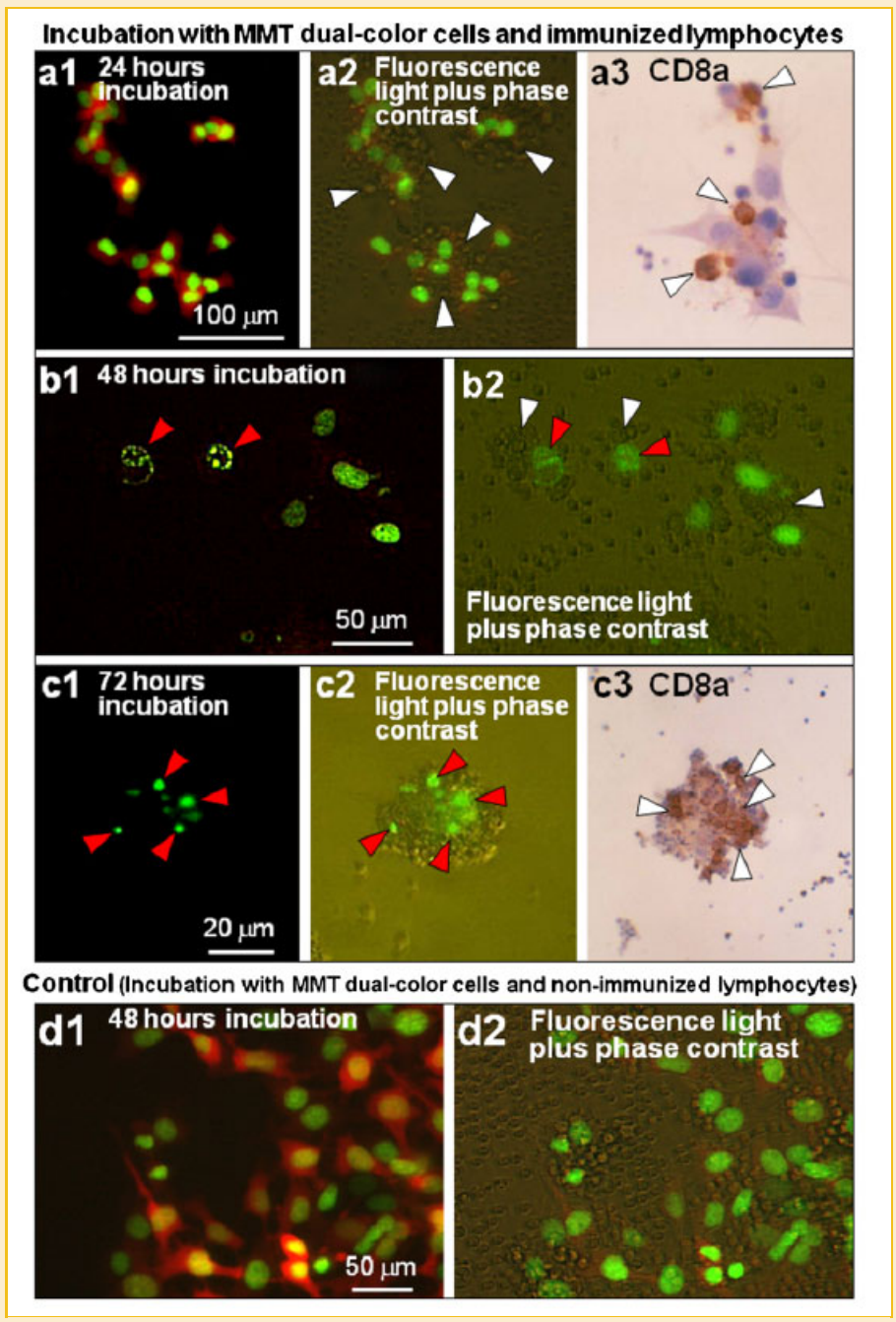

Fig. 5. In vitro interaction of the dual-colored MMT cells and sensitized lymphocytes, derived from ND-GFP transgenic immunocompetent mice with MMT tumors, was visualized. a1–a3: After 24 h, many lymphocytes attached to the cancer cells (a2) (white arrowheads). The lymphocytes that attached to the cancer cells were CD8a-positive (a3) (white arrowheads). b,c: After 48 h (b1,b2), and 72 h (c1–c3), GFP-expressing cancer cell nuclei had condensed chromatin (red arrowheads). The lymphocytes that attached to the cancer cells were CD8a-positive (c3) (white arrowheads). (d1,d2) 48 h co-incubation of dual-colored MMT cells and nonimmunized lymphocytes from ND-GFP transgenic immunocompetent mice. The dual-colored MMT cells looked and grew normally without apoptosis.

cell nuclei had ring-shaped chromatin condensation (Fig. 4c,d). At day-4, apoptotic cells appeared in the tumor. Transmission electron microscopy showed that the cancer cells displayed apoptotic characteristics, including chromatin condensation, nuclear fragmentation, and apoptotic body formation (Fig. 4e,f). At day-6, MMT nuclei were observed to partition from the cytoplasm of dual-color MMT cells. The partitioned chromatin had the appearance of a thread-like structure of nuclear material. The cancer cells contained irregularly elongated nuclei. The nuclear membranes of the cancer cells ruptured, and nuclear material extruded (Fig. 4g,h). At day-7, T lymphocytes were observed to infiltrate into the tumor mass in ND-GFP immunocompetent mice. CD3ε-, CD8a-, and granzyme B-positive T lymphocytes infiltrated the tumor (data not shown).

INTERACTION OF MMT CELLS AND IMMUNIZED LYMPHOCYTES IN VITRO

Dual-color MMT cells were co-cultured in vitro along with lymphocytes obtained from mice with MMT tumors. After 24 h incubation, many lymphocytes attached to the cancer cells. The lymphocytes that attached to the cancer cells at 24 h were CD8a-positive. Between 48 and 72 h co-culture, condensation of chromatin in cancer-cell nuclei commenced. After 48 h incubation of MMT cells with nonimmunized lymphocytes, the cancer cells looked and grew normally (Fig. 5).

The use of ND-GFP transgenic mice as hosts, in which nascent blood vessels express GFP and dual-color MMT cells in which the cytoplasm expresses RFP and the nuclei express GFP, allowed very important novel angiogenesis and subcellular death-pathway observations to be made during immune rejection of a tumor. Nascent blood vessels did not form in the initially-growing mouse mammary tumor in immunocompetent mice. In contrast, in nude mice, numerous nascent blood vessels grew into the tumor. The results suggest that insufficient nascent tumor angiogenesis was important in tumor rejection. During immune rejection, the cancer cells had deformed cytoplasm and nuclei which partitioned. The nuclear membranes of the cancer cells ruptured, and chromatin extruded during partitioning of cytoplasm and nuclei. Immune cells appeared to have an important role in tumor rejection. The cytotoxic role of the T lymphocytes was confirmed in vitro in co-culture with MMT cells. The color-coded fluorescence subcellular imaging model of immune rejection of cancer cells provides a comprehensive system for further testing of immune-based treatment for cancer.

REFERENCES

Amoh Y, Li L, Yang M, Moossa AR, Katsuoka K, Penman S, Hoffman RM. 2004. Nascent blood vessels in the skin arise from nestin-expressing hair-follicle cells. Proc Natl Acad Sci USA 101:13291–13295.

Amoh Y, Yang M, Li L, Reynoso J, Bouvet M, Moossa AR, Katsuoka K, Hoffman RM. 2005. Nestin-linked green fluorescent protein transgenic nude mouse for imaging human tumor angiogenesis. Cancer Res 65:5352–5357.

Bouvet M, Tsuji K, Yang M, Jiang P, Moossa AR, Hoffman RM. 2006. In vivo color-coded imaging of the interaction of colon cancer cells and splenocytes in the formation of liver metastases. Cancer Res 66:11293–11297.

Duda DG, Duyverman AM, Kohno M, Snuderl M, Steller EJ, Fukumura D, Jain RK. 2010. Malignant cells facilitate lung metastasis by bringing their own soil. Proc Natl Acad Sci USA 107:21677–21682.

Hayashi K, Jiang P, Yamauchi K, Yamamoto N, Tsuchiya H, Tomita K, Moossa AR, Bouvet M, Hoffman RM. 2007. Real-time imaging of tumor-cell shedding and trafficking in lymphatic channels. Cancer Res 67:8223–8228.

Hoffman RM. 2005. The multiple uses of fluorescent proteins to visualize cancer in vivo. Nat Rev Cancer 5:796–806.

Hoffman RM, Yang M. 2006. Subcellular imaging in the live mouse. Nat Protoc 1:775–782.

Jiang P, Yamauchi K, Yang M, Tsuji K, Xu M, Maitra A, Bouvet M, Hoffman RM. 2006. Tumor cells genetically labeled with GFP in the nucleus and RFP in the cytoplasm for imaging cellular dynamics. Cell Cycle 5:1198–1201.

Li L, Mignone J, Yang M, Matic M, Penman S, Enikolopov G, Hoffman RM. 2003. Nestin expression in hair follicle sheath progenitor cells. Proc Natl Acad Sci USA 100:9958–9961.

Tsuji K, Yamauchi K, Yang M, Jiang P, Bouvet M, Endo H, Kanai Y, Yamashita K, Moossa AR, Hoffman RM. 2006. Dual-color imaging of nuclear-cytoplasmic dynamics, viability, and proliferation of cancer cells in the portal vein area. Cancer Res 66:303–306.

Yamamoto N, Jiang P, Yang M, Xu M, Yamauchi K, Tsuchiya H, Tomita K, Wahl GM, Moossa AR, Hoffman RM. 2004. Cellular dynamics visualized in live cells in vitro and in vivo by differential dual-color nuclear-cytoplasmic fluorescent-protein expression. Cancer Res 64:4251–4256.

Yamauchi K, Yang M, Jiang P, Yamamoto N, Xu M, Amoh Y, Tsuji K, Bouvet M, Tsuchiya H, Tomita K, Moossa AR, Hoffman RM. 2005. Real-time in vivo dual-color imaging of intracapillary cancer cell and nucleus deformation and migration. Cancer Res 65:4246–4252.

Yang M, Reynoso J, Jiang P, Li L, Moossa AR, Hoffman RM. 2004. Transgenic nude mouse with ubiquitous green fluorescent protein expression as a host for human tumors. Cancer Res 64:8651–8656.

Yang M, Jiang P, Hoffman RM. 2007. Whole-body subcellular multicolor imaging of tumor-host interaction and drug response in real time. Cancer Res 67:5195–5200.